Morphology and Ionic Conductivity of Polymer Complexes Formed by Segmented Polyether Poly(urethane urea) and Lithium Perchlorate

Masayoshi Watanabe,*[1a] Shin-ichiro Oohashi,[1a] Kohei Sanui,[1a] Naoya Ogata,[1a] Tadahiko Kobayashi,[1b] and Zentaro Ohtaki[1b]

Department of Chemistry and Department of Electrical and Electronic Engineering, Sophia University, Kioi-cho, Chiyoda-ku, Tokyo 102, Japan. *Received December 10, 1984*

ABSTRACT: Segmented polyether poly(urethane ureas) (PEUU) were synthesized from 4,4′-methylenebis(phenyl isocyanate), ethylenediamine, and poly(propylene oxide) with molecular weight of either 2000 or 3000. Lithium perchlorate ($LiClO_4$) was dissolved in the PEUU's by immersing the polymer in an acetone solution of the salt. The correlation between the morphology and the ion-conducting behavior of the PEUU·$LiClO_4$ complexes was investigated. The salt-free PEUU's appear to form a two-phase structure composed of a continuous polyether phase and an isolated poly(urethane urea) phase. $LiClO_4$ is selectively dissolved in the polyether phase. The dissolution of $LiClO_4$ considerably increases the T_g of the polyether segment. Complex impedance diagrams of the bulk impedance of PEUU·$LiClO_4$ complexes were interpreted in terms of an equivalent circuit based on their morphology. Ionic conductivity was influenced by the $LiClO_4$ concentration and the molecular weight of the polyether segment. An equation consisting of a superposition of the Williams–Landel–Ferry type equation for ionic mobility and the Arrhenius type equation for number of carrier ions was suitable for interpreting the temperature dependence of the ionic conductivity.

Introduction

Segmented polyether poly(urethane ureas) (PEUU) are known to be typical thermoplastic elastomers.[2] These polymers have the general structure $(A–B)_x$, where A is a poly(urethane urea) segment (hard segment) and B is a polyether segment (soft segment). Their favorable properties as thermoplastic elastomers are based on their distinct two-phase microstructure. At a given temperature, the soft segment is in the rubbery state, whereas the hard segment is in the glassy or semicrystalline state. Thus, the hard-segment domains operate not only as physical cross-linking points but also as hard fillers.

As the soft segment, poly(ethylene oxide) (PEO), poly(propylene oxide) (PPO), and poly(tetramethylene oxide) are often used. PEO and PPO have the same backbone structure as the macrocyclic polyethers ("crown ethers"). Alkali metal salts dissolve in these polymers to a high concentration without forming ionic multiplets or ionic clusters,[3,4] which seems to be caused by cooperative interaction of neighboring ether oxygens and ions, as seen in the macrocyclic polyether. Furthermore, high segmental mobility of these polyethers, corresponding to low glass transition temperatures (T_g), ensures high mobility of the dissociated ions. Thus, the polymer complexes formed by the polyethers and alkali metal salts show a relatively high ionic conductivity.[5–12]

It has recently been reported that an alkali metal salt (NaSCN) complexes selectively with PEO sements in a PEO–polyisoprene (PI)–PEO block copolymer.[13] The thermal and mechanical properties were remarkably altered by the complexation. If alkali metal salts selectively complex with the polyether segment of PEUU's in a similar manner as seen in the PEO–PI–PEO block copolymer, it may be expected that electrical properties as well as thermal and mechanical properties are changed by the complexation.

In this study, we intended to obtain ion-conducting PEUU's. PEUU's composed of 4,4′-methylenebis(phenyl isocyanate) (MDI), ethylenediamine (ED), and PPO (MW = 2000 or 3000) were synthesized. The weight percent of the hard segment in the PEUU's was kept at 30% in order to make a continuous PPO phase conduction path. Lithium perchlorate ($LiClO_4$) was dissolved in the PEUU's by an immersion method. The morphology of the PEUU·$LiClO_4$ complexes was investigated by using infrared (IR) spectra, differential scanning calorimetry (DSC), and dynamic mechanical measurements. An impedance technique was used for electrical measurements. An equivalent circuit suitable for interpreting the impedance results was employed, taking the morphology into consideration. Ionic conductivity, estimated from the corresponding component of the equivalent circuit, was influenced by the $LiClO_4$ concentration and the molecular weight of the PPO segment. The temperature dependence of the ionic conductivity was evaluated in terms of the ionic mobility and the number of carrier ions.

Scheme I
Synthesis of Segmented Polyether Poly(urethane ureas)

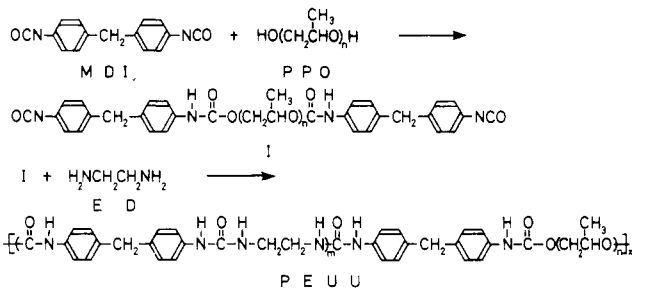

Experimental Section

A. Synthesis. PEUU's were synthesized by a two-step addition reaction according to Scheme I.

MDI (Wako Pure Chemical Ind. Ltd.) was vacuum-distilled (200 °C (9 mmHg)). PPO (Asahi Denka Ind. Ltd.) was dehydrated under reduced pressure at 80 °C for 8 h. ED (Wako Pure Chemical Ind. Ltd.) was refluxed over metallic sodium (3 wt %) for 2 h and distilled. *N,N*-Dimethylacetamide (DMAc) (Wako Pure Chemical Ind. Ltd.) was dehydrated by 4A molecular sieves and vacuum-distilled.

A mixture of PPO and MDI was allowed to react at 80 °C for 8 h with stirring. The contents were cooled to room temperature, and DMAc was added to form a homogeneous solution. The solution was cooled to −5 °C and a DMAc solution of ED (10 wt %) was added. The total concentration of reactants in the solution was about 20 wt %. Polymerization proceeded at −5 °C for 1.5 h with stirring. Throughout the course of the synthesis the reactants were purged by dry nitrogen. The polymers were precipitated by using a large excess of methanol and dried under

0024-9297/85/2218-1945$01.50/0

Table I
Characterization of Segmented Polyether Poly(urethane ureas)

desig	molar ratio MDI/ED/PPO	M_n(PPO)	wt % of hard segment	wt % of ED	elem anal.[b] % C	% H	% N	$(\eta_{sp}/C)/(dL/g)$[a]
PEUU-3000	4/3/1	2833	29	5.0	63.5 (63.3)	8.9 (8.9)	4.7 (4.9)	0.69
PEUU-2000	3/2/1	2010	29	4.0	63.4 (63.3)	8.9 (8.9)	4.7 (4.7)	0.81

[a] Measured in *N,N*-dimethylformamide at 0.1 g/10 cm^3 at 30 °C. [b] Values in parentheses are calculated.

a reduced pressure at 80 °C for 5 days. Characteristics of the sample are summarized in Table I. The numeral in the polymer designation represents the number-average molecular weight of the PPO segment. The molar ratio of MDI, ED, and PPO was altered for the different molecular weight PPO's in order to keep the weight percent of the hard segment at 30 wt %.

Films for various measurements were prepared by casting a DMAc solution of PEUU onto glass substrates, followed by evaporating the solvent at 70 °C. The films obtained were dried completely under reduced pressure at 80 °C for 4 days.

B. Dissolution of $LiClO_4$. A special grade anhydrous $LiClO_4$ (Mitsuwa Kagaku Ltd.) was dried under reduced pressure (10^{-3} torr) at 180 °C for 8 h. Acetone was dehydrated by 4A molecular sieves and distilled. Since PEUU films were swollen by an acetone solution of $LiClO_4$, an immersion method was used for dissolution of $LiClO_4$ in PEUU's. A preweighed PEUU film was immersed in an acetone solution of $LiClO_4$ and was dried under reduced pressure at 80 °C for 2 days. In order to ensure a uniform dissolution of $LiClO_4$ through the film thickness, the immersing was continued till the weight change of the dried film before and after the immersing reached a constant level. Thus, the concentration of $LiClO_4$ in PEUU's was controlled by changing the concentration of the immersion solutions and was determined from the weight change of the film before and after the immersing. It was previously confirmed that a weight change did not occur when a PEUU film was immersed in acetone followed by drying. The concentration of $LiClO_4$ in the PEUU·$LiClO_4$ complexes was represented by the molar ratio of $LiClO_4$ to the repeating unit of PPO ([$LiClO_4$]/[PO unit]). The exclusion of water and acetone from the PEUU·$LiClO_4$ complexes was checked by the absence of absorptions around 3450 cm^{-1} and at 1720 cm^{-1} in the IR spectra.

C. Method. IR spectra were measured by using a Hitachi 260-50 spectrophotometer. Samples used were thin films (about 0.02 mm thick). Positions of the characteristic bands were calibrated by using standard bands of polystyrene. DSC measurements over the temperature ranges of −160 to +100 and +40 to +350 °C were carried out by using a low-temperature type and a standard type DSC apparatus (Rigaku Denki 8085), respectively, at a heating rate of 20 °C/min. The glass transition zone was determined as the temperature range between two intersection points of the base lines with the extrapolated sloping portion of the thermogram, which resulted from a heat capacity change, as shown in Figure 2 by dashed lines. T_g was defined as the midpoint of the heat capacity change. Dynamic mechanical measurements were made with a Toyo Rheovibron DDV-II at 11 Hz at a heating rate of 2 °C/min.

Impedance measurements were performed as follows. A disk-like film (13-mm diameter and 0.5 mm thick) sandwiched between two electrodes (13-mm diameter) was packed in a sealed cell under a dry argon atmosphere. Ribbon-like metallic lithium (Alpha Products, 19-mm width, 0.75 mm thick) was cut into disks, which were used as lithium electrodes. The frequency dependence of the cell impedance was measured with a Hewlett-Packard 4800A vector impedance meter equipped with a Takeda Riken TR5821 universal counter.

PEUU·$LiClO_4$ complexes were handled in an inert atmosphere in order to exclude traces of water.

Results and Discussion

A. Morphological Study. Since hard segments of PEUU's are generally found to be extensively hydrogen bonded, an analysis of the IR spectra of PEUU's and PEUU·$LiClO_4$ complexes may provide detailed information about changes in morphology with the dissolution of $LiClO_4$. Thus, an IR analysis was carried out, on the basis of the resolution of the NH and carbonyl bands for urethane and urea linkages into hydrogen-bonded and free components. Figure 1 shows the IR spectra of PEUU-3000 and PEUU-3000·$LiClO_4$ complex. PEUU-3000 showed the characteristic bands for the NH and carbonyl absorptions at 3320, 1730, 1705, and 1635 cm^{-1}. Wang and Cooper[2] recently reported that PEUU's consisting of MDI, ED, and poly(tetramethylene oxide) showed free NH absorption at 3445 cm^{-1}, hydrogen-bonded NH absorption at 3305–3320 cm^{-1}, free urethane carbonyl absorption at 1731–1732 cm^{-1}, hydrogen-bonded urethane carbonyl absorption at 1705–1710 cm^{-1}, free urea carbonyl absorption at 1695 cm^{-1}, and hydrogen-bonded urea carbonyl absorption at 1635–1645 cm^{-1}. Considering the results of Wang and Cooper[2] and other workers,[14] we assigned the absorptions at 3320, 1730, 1705, and 1635 cm^{-1} to the bonded ν_{NH} band, the free urethane $\nu_{C=O}$ band, the bonded urethane $\nu_{C=O}$ band, and the bonded urea $\nu_{C=O}$ band, respectively. Thus, it was revealed that all the NH and carbonyl groups of the urea linkage in the hard segments were hydrogen bonded with each other. This fact reflects the aggregation of the hard segments and two-phase structure of the PEUU. As for the urethane linkage, all of the NH groups and a part of the urethane carbonyl groups were hydrogen bonded. Since the PEUU had the chemical structure shown in

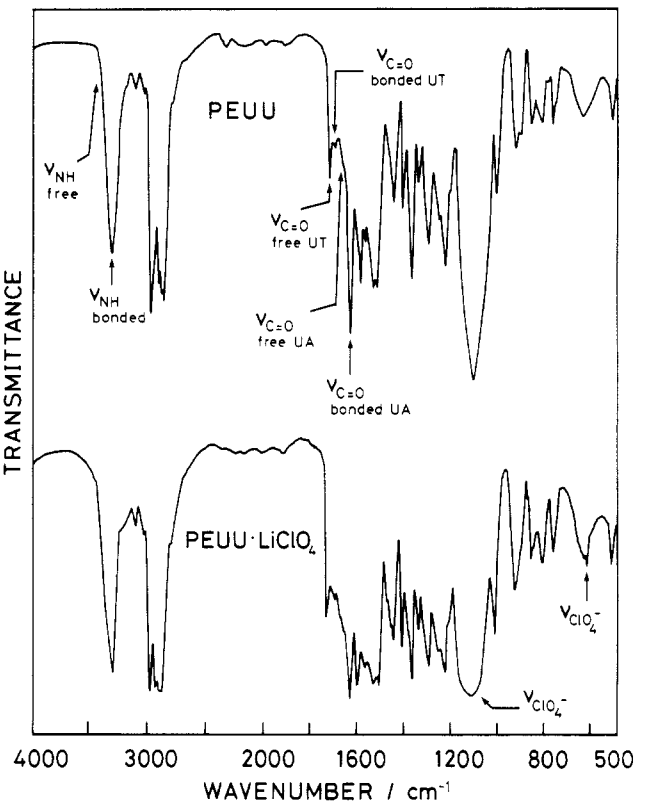

Figure 1. Infrared spectra of PEUU-3000 and PEUU-3000·$LiClO_4$ complex ([$LiClO_4$]/[PO unit] = 0.03).

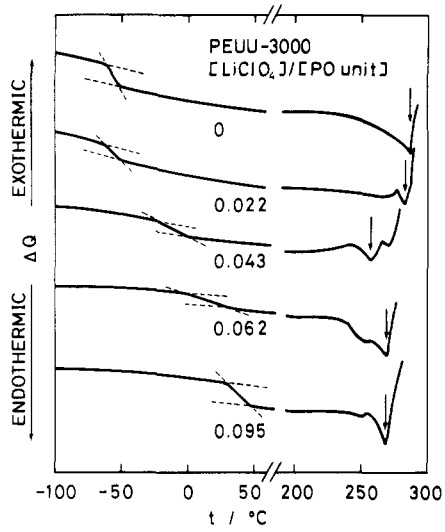

Figure 2. Differential scanning calorimetry curves of PEUU-3000 and PEUU-3000·$LiClO_4$ complexes with various $LiClO_4$ concentrations.

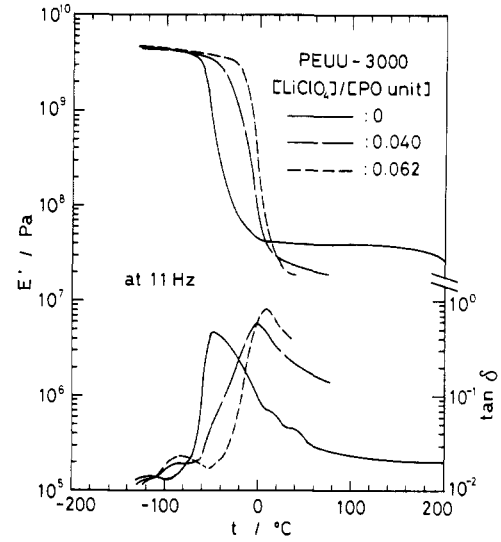

Figure 3. Storage elastic modulus and dissipation factor as a function of temperature for PEUU-3000 and PEUU-3000·$LiClO_4$ complexes with various $LiClO_4$ concentrations.

Table II
Thermal Properties of PEUU and PEUU·$LiClO_4$ Complexes

$[LiClO_4]$/[PO unit]	T_g (range)/°C	ΔT_g/°C	T_m/°C
	PEUU-3000		
0	−58 (−62 to −53)	9	287
0.015	−58 (−62 to −53)	9	275
0.022	−57 (−63 to −52)	11	283
0.040	−21 (−40 to −1)	39	258
0.043	−10 (−22 to 2)	24	257
0.062	12 (−4 to 27)	31	269
0.095	38 (29 to 46)	17	268
	PEUU-2000		
0	−52 (−56 to −47)	9	287
0.025	−37 (−43 to −27)	16	279
0.044	−2 (−27 to 12)	39	262

Scheme I, these absorptions may originate from urethane linkages that exist in the vicinity of the interface between hard and soft segments.

The spectrum of the PEUU-3000·$LiClO_4$ complex showed qualitatively a similar profile to that of the salt-free PEUU-3000, except for the broadness of the absorption around 1110 cm^{-1} and the absorption at 620 cm^{-1}. These two bands could be assinged to the stretching modes of ClO_4^-.[15] Free NH and free urea carbonyl absorptions were not observed, which indicated that the hard segments are hydrogen bonded with each other similarly to those of the salt-free PEUU-3000. Thus, $LiClO_4$ may dissolve selectively in the polyether phase. These results were also observed in the PEUU-2000 series.

Figure 2 shows the DSC thermograms of PEUU-3000 and the PEUU-3000·$LiClO_4$ complexes with various $LiClO_4$ concentrations. The results of the DSC analysis are summarized in Table II. In salt-free PEUU-3000, the T_g of the soft segment and the melting point (T_m) of the hard segment appeared at −58 and 287 °C, respectively. With increasing $LiClO_4$ concentration from 0 to about 0.1, T_g of the soft segment increased by about 100 °C, whereas T_m of the hard segment decreased at most by 30 °C. Moacanin et al.[4] reported that the T_g of PPO increased considerably with increasing $LiClO_4$ concentration. They interpreted the increase in T_g by assuming that PPO with dissolved $LiClO_4$ is a copolymer of complexed propylene oxide (PO) units with $LiClO_4$ and pure PO units. The complexed PPO has a high T_g. The increase in T_g is due to a change in the copolymer composition with increasing $LiClO_4$ concentration. Thus the increase in T_g of the PPO segment in the present system is clear evidence that $LiClO_4$ dissolves selectively in the PPO phase. The glass transition zone (ΔT_g) had a maximum at a $LiClO_4$ concentration of $[LiClO_4]/[PO\ unit] = 0.04$. Complexed PO units may be located randomly along the PPO segment. The superposition of the behavior of the free and complexed PO units may be responsible for the wider distribution of the relaxation times. This might make the glass transition zone large. At a higher $LiClO_4$ concentration almost all PO units are complexed with $LiClO_4$, and thus the distribution of the relaxation times becomes narrow again.

The T_g of the PPO segment of salt-free PEUU-2000 was −52 °C, which was higher than that of PEUU-3000. With increasing $LiClO_4$ concentration, the T_g of the PPO segment increased in a similar manner to the behavior observed in the PEUU-3000 series. At the same $LiClO_4$ concentration, the T_g's were somewhat higher in the PEUU-2000 series.

Figure 3 shows the storage elastic modulus (E') and the dissipation factor (tan δ) as a function of temperature for the PEUU-3000 series. The behavior of salt-free PEUU-3000, which showed a rubbery plateau level of 4×10^7 Pa over a wide temperature range (0–200 °C), was characteristic of a typical thermoplastic elastomer with a two-phase morphology. The main peak in tan δ corresponded to T_g of the PPO segment. When $LiClO_4$ was dissolved in the PEUU, the dynamic mechanical property could not be measured over a wide temperature range because the samples became brittle. However, the notable change was high-temperature shifts of the E' relaxations and tan δ peaks, corresponding to the backbone motion of the PPO segments. The profile of the tan δ peak was relatively sharp for the salt-free sample. The profile became broad when the salt concentration was 0.040, and it became sharp again when the salt concentration was 0.062. In agreement with the DSC results, these temperature shifts and profile changes indicate the selective dissolution of $LiClO_4$ in the PPO phase.

B. Complex Impedance Study. It is known that the bulk impedance of an ionic conductor, excluding the contribution of interfacial impedance between an ionic conductor and electrodes, can be obtained by the complex impedance method.[16] In order to separate the bulk and interfacial impedances, complex impedance measurements

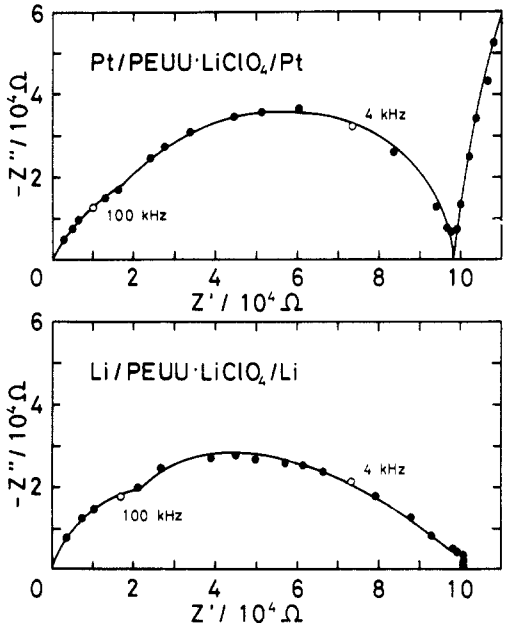

Figure 4. Complex impedance diagrams of PEUU-3000·$LiClO_4$ complex ([$LiClO_4$]/[PO unit] = 0.040) sandwiched between either platinum or lithium electrodes at 68 °C.

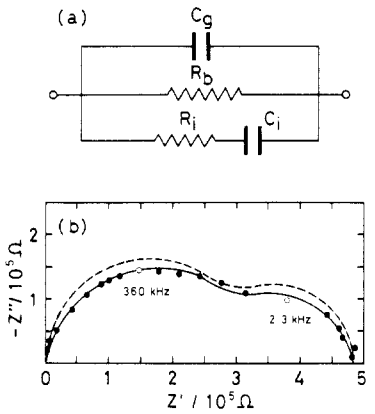

Figure 5. Equivalent circuit to interpret complex impedance diagrams (a) and complex impedance diagram of PEUU-3000·$LiClO_4$ complex ([$LiClO_4$]/[PO unit] = 0.015) sandwiched between platinum electrodes at 69 °C (b). Meanings of C_g, R_b, C_i, and R_i are cited in the text. The simulated complex impedance diagram is indicated by a dashed line.

on different electrode cells were carried out. Figure 4 shows the complex impedance diagrams of the PEUU-3000·$LiClO_4$ complex sandwiched between either platinum or lithium electrodes. The main difference in the diagrams was the low-frequency behavior: the complex impedance diagram for the cell with platinum electrodes had a low-frequency spur, whereas this feature was missing in the cell with lithium electrodes. These differences are attributed to differences in the interfacial impedance. Platinum functions as an ion-blocking electrode, whereas lithium functions as an ion-reversible electrode toward the sample. Thus we can extract the bulk impedance loci from the complex impedance diagrams. The bulk impedance loci appeared to be a superposition of two semicircles having different time constants. We suspected that this profile is based on the microstructure of the sample.

As mentioned in the previous section, the PEUU's had a two-phase structure in which the polyether phase is continuous and the poly(urethane urea) phase is isolated. $LiClO_4$ was dissolved selectively in the polyether phase. Taking this morphology into consideration, we assume an equivalent circuit in order to interpret the profile of the bulk impedance loci, as shown in Figure 5a. C_g means geometrical capacitance, determined by the dielectric constant and geometry of the sample. R_b means bulk resistance of the sample, which corresponds to the continuous polyether paths with dissolved $LiClO_4$. Series combination of R_i and C_i means the paths in which migration of carrier ions in the polyether paths is blocked by the poly(urethane urea) phase. Thus, C_i may correspond to the interfacial capacitance between the polyether and poly(urethane urea) phase, and R_i may coincide roughly with R_b. In order to confirm validity of the assumed equivalent circuit, we simulated the complex impedance diagram, as shown in Figure 5b. The frequency dependence of the impedance of the equivalent circuit is represented by

$$Z = \frac{R_b(1 + i\omega C_i R_i)}{(1 - \omega^2 C_g C_i R_b R_i) + i\omega(C_i R_i + C_i R_b + C_g R_b)} \quad (1)$$

The dashed line in the figure is the simulated diagram obtained with eq 1 and the values in Table III. The simulated diagram expressed fairly well the experimentally obtained diagram. R_b and R_i were not very different from each other. C_i was somewhat greater than C_g. We could also simulate the other impedance diagrams at different temperatures and at different salt concentrations by using the equivalent circuit. Thus we concluded that the characteristic profile of the bulk impedance diagrams was based on the morphology of the PEUU·$LiClO_4$ complexes.

Table III
Parameters To Simulate Complex Impedance Diagram by Using an Equivalent Circuit

C_g/F	R_b/Ω	C_i/F	R_i/Ω
2.0×10^{-11}	4.8×10^5	5.0×10^{-11}	1.0×10^6

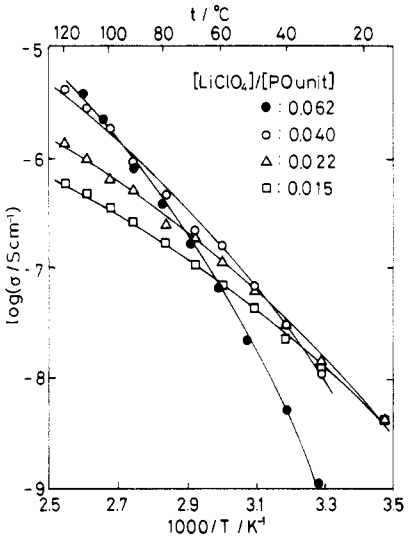

Figure 6. Temperature dependence of ionic conductivity for PEUU-3000·$LiClO_4$ complexes with various $LiClO_4$ concentrations.

C. Temperature Dependence of Ionic Conductivity. Figure 6 shows the temperature dependence of ionic conductivity for the PEUU-3000·$LiClO_4$ complexes with various $LiClO_4$ concentrations. The ionic conductivity was calculated from the bulk resistance found in the complex impedance diagrams. The temperature dependence did not obey the Arrhenius theory with a constant activation energy but was expressed experimentally by a Williams–Landel–Ferry (WLF) type equation[17,18]

$$\log \frac{\sigma(T)}{\sigma(T_g)} = \frac{C_1(T - T_g)}{C_2 + (T - T_g)} \quad (2)$$

Table IV
WLF Parameters of PEUU•$LiClO_4$ Complexes

$[LiClO_4]$/[PO unit]	T_g/°C	C_1	C_2/°C	$\sigma(T_g)$/(S cm^{-1})
		PEUU-3000		
0.015	−58	13.5	39.4	5.8×10^{-18}
0.022	−57	13.7	50.9	3.0×10^{-17}
0.040	−21	10.7	82.0	8.1×10^{-13}
0.062	12	10.1	97.9	2.5×10^{-11}
		PEUU-2000		
0.025	−37	10.6	54.2	1.0×10^{-14}
0.044	−2	9.3	91.1	1.4×10^{-11}

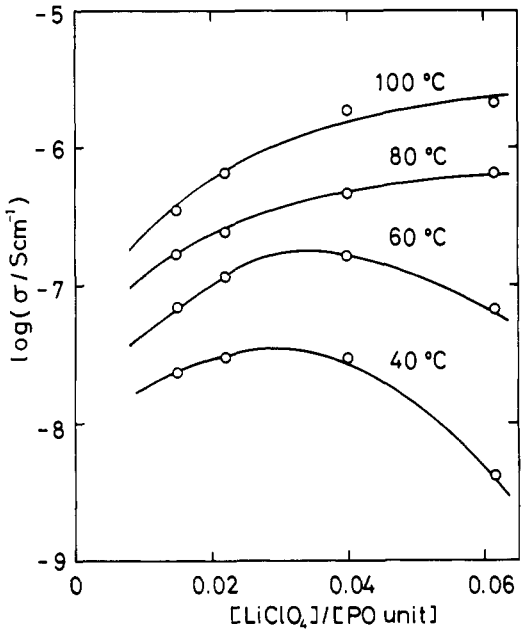

Figure 7. Ionic conductivity as a function of $LiClO_4$ concentration for PEUU-3000•$LiClO_4$ complexes at various temperatures.

by using the parameters shown in Table IV. This fact implied that the segmental motion of the PPO main chain cooperates with the carrier motion and that the temperature dependence is dominated by that of the ionic mobility (μ). However, the WLF parameters of C_1 and C_2 deviated considerably from the standard values[17] (C_1 = 17.4, C_2 = 51.6) for the temperature dependence of the segmental mobility with increasing $LiClO_4$ concentration. The conductivity data in Figure 6 are replotted against the $LiClO_4$ concentration in Figure 7. The conductivity as a function of $LiClO_4$ concentration was somewhat complicated; that is, the conductivity tended to decrease with increasing concentration at 40 °C, whereas the conductivity increased with increasing concentration at 100 °C. Thus these conductivity data could not be explained by only the effect of μ or by only the effect of the number of carrier ions (n).

We have already presented the equation that expresses quantitatively the temperature dependence of the ionic conductivity of the polymer complex formed by PPO–urethane networks and $LiClO_4$ above their T_g's.[12] The equation is

$$\sigma = \frac{e^2 N_0 D_0}{kT} \exp\left[-\left(\frac{U/2\epsilon}{kT} + \frac{\gamma V_i^*}{V_f}\right)\right] \quad (3)$$

where e is the elementary electric charge, N_0 and D_0 are constants, k is the Boltzmann constant, U is the dissociation energy of ion pairs, ϵ is the relative dielectric constant, γ is a numeric factor, V_i^* is the critical volume

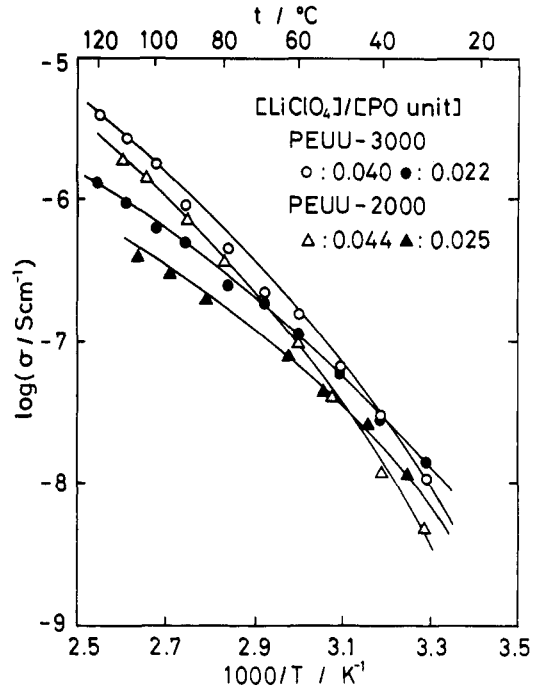

Figure 8. Temperature dependence of ionic conductivity for PEUU-3000•$LiClO_4$ and PEUU-2000•$LiClO_4$ complexes with various $LiClO_4$ concentrations.

required for the migration of carrier ions, and V_f is the free volume. Equation 3 is based on the changed μ and n as follows:

$$\mu = \frac{eD_0}{kT} \exp\left(-\frac{\gamma V_i^*}{V_f}\right) = \frac{eD_0}{kT} \exp\left[\frac{-\gamma V_i^*}{V_g\{f_g + \alpha(T - T_g)\}}\right] \quad (4)$$

$$n = N_0 \exp\left(-\frac{U/2\epsilon}{kT}\right) \quad (5)$$

where V_g is the specific volume at T_g, f_g is the fractional free volume at T_g, and α is the expansion coefficient of free volume. The WLF type equation (eq 2) can be derived from eq 4, assuming that the temperature dependence of n is negligible. Thus eq 3 is a superposition of the WLF type equation for μ and the Arrhenius type equation for n. The conductivity data of the PEUU•$LiClO_4$ complexes were explained by using eq 3. The μ values at the same temperature seem to decrease with increasing $LiClO_4$ concentration, since the main contributing term to μ in eq 4 is $T - T_g$ and the other terms do not seem to change so much with $LiClO_4$ concentration. On the other hand, the activation energy in eq 5 may increase with increasing $LiClO_4$ concentration. We could understand the conductivity data in Figures 6 and 7 by combining these two effects. The main contributing term to the difference in the conductivity at lower temperatures may be μ, since $T - T_g$ for each sample was very different, depending on the $LiClO_4$ concentration. At higher temperatures the term $T - T_g$ does not change as greatly with the concentration as it does at lower temperatures. This may result in similar μ values. Thus the conductivity may be determined by the difference of n. Increasing activation energy for n with increasing $LiClO_4$ concentration might make higher n values.

Figure 8 is a comparison of the conductivity between PEUU-3000•$LiClO_4$ and PEUU-2000•$LiClO_4$ complexes at

nearly the same $LiClO_4$ concentrations. The conductivity was higher in the PEUU-3000·$LiClO_4$ complex at the same concentration, whereas profiles of the temperature dependence were similar. The latter fact is also confirmed by the similar WLF parameters, as shown in Table IV. In this case the activation energy for n is considered to be the same. Therefore the difference in the conductivity is assumed to be determined by that in μ. T_g's of the PEUU-2000·$LiClO_4$ complexes were higher than those of the PEUU-3000·$LiClO_4$ complexes. The higher T_g's in the PEUU-2000·$LiClO_4$ complexes result in the lower μ values.

References and Notes

(1) (a) Department of Chemistry. (b) Department of Electrical and Electronic Engineering.
(2) For example: Wang, C. B.; Cooper, S. L. *Macromolecules* **1983**, *16*, 775.
(3) Santaniello, E.; Manzocchi, A.; Sozzani, P. *Tetrahedron Lett.* **1979**, *47*, 4581.
(4) Moacanin, J.; Cuddihy, E. F. *J. Polym. Sci., Part C* **1966**, *14*, 313.
(5) Wright, P. V. *Br. Polym. J.* **1975**, *7*, 319.
(6) Armand, M. B.; Chabagno, J. M.; Duclot, M. J. In "Fast Ion Transport in Solids"; Vashishta, P., Mundy, J. N., Shenoy, G. K., Eds.; North-Holland Publishing Co.: Amsterdam, 1979; pp 131-136.
(7) Dupon, R.; Papke, B. L.; Ratner, M. A.; Whitmore, D. H.; Shriver, D. F. *J. Am. Chem. Soc.* **1982**, *104*, 6247.
(8) Killis, A.; LeNest, J. F.; Cheradame, H.; Gandini, A. *Makromol. Chem.* **1982**, *183*, 2835.
(9) Watanabe, M.; Nagaoka, K.; Kanba, M.; Shinohara, I. *Polym. J. (Tokyo)* **1982**, *14*, 877.
(10) Watanabe, M.; Ikeda, J.; Shinohara, I. *Polym. J. (Tokyo)* **1983**, *15*, 65.
(11) Watanabe, M.; Ikeda, J.; Shinohara, I. *Polym. J. (Tokyo)* **1983**, *15*, 175.
(12) Watanabe, M.; Sanui, K.; Ogata, N.; Kobayashi, T.; Ohtaki, Z. *J. Appl. Phys.* **1985**, *57*, 123.
(13) Robitaille, C.; Prud'homme, J. *Macromolecules* **1983**, *16*, 665.
(14) Sung, C. S. P.; Smith, T. W.; Sung, N. H. *Macromolecules* **1980**, *13*, 117.
(15) Cohen, H. *J. Chem. Soc.* **1952**, 4282.
(16) (a) Macdonald, J. R. *J. Chem. Phys.* **1973**, *58*, 4982. (b) Macdonald, J. R. *J. Chem. Phys.* **1974**, *61*, 3977.
(17) Williams, M. L.; Landel, R. F.; Ferry, J. D. *J. Am. Chem. Soc.* **1955**, *77*, 3701.
(18) Sasabe, H.; Saito, S. *Polym. J. (Tokyo)* **1972**, *3*, 624.

Calculation of the Fourth-Order Correlation Function of a Polymer Coil (As Measured by Cross-Correlation Light Scattering)

P. N. Pusey*

Department of Physics, University of Colorado, Boulder, Colorado 80309.

Received November 14, 1984

ABSTRACT: We calculate some properties of $f^{(4)}(\mathbf{K},\mathbf{Q},\tau)$, the normalized fourth-order correlation function of the electric field amplitude of light scattered by a *single* isolated polymer coil. This quantity can be measured in an experiment where the light intensities scattered in two directions (defined by scattering vectors $\mathbf{K}$ and $\mathbf{Q}$) by a *small volume* of a *dilute* polymer solution are cross correlated. As expected $f^{(4)}$, which describes conformational fluctuations of the polymer coil, contains more information than the second-order function usually measured in dynamic light scattering experiments. We consider both the amplitude $f^{(4)}(\mathbf{K},\mathbf{Q},0)$ of the conformational fluctuations and their initial time dependence $\lim_{\tau\to 0}[\mathrm{d}f^{(4)}(\mathbf{K},\mathbf{Q},\tau)/\mathrm{d}\tau]$. This work provides a theoretical basis for a recent experiment of Kam and Rigler (*Biophys. J.* **1982**, *39*, 7-13) as well as suggesting some new experiments.

I. Introduction

In this paper we consider the theory underlying an experiment[1] in which fluctuations in the light scattered by a small volume of a dilute solution of random-coil polymers are analyzed by a cross-correlation technique. In this situation, where the volume contains on average a relatively small number of macromolecules, conformational fluctuations (i.e., changes in the instantaneous shape) of the polymer coils modulate the "number fluctuation term" (see below) in the temporal correlation function of the scattered light intensity. As we will show explicitly in section II, the function describing these conformational fluctuations (eq 2.17) is essentially the *correlation function of the intensity scattered by a single polymer coil* or, equivalently, the *fourth-order* correlation function of the scattered light field. Thus this type of experiment provides, in principle at least, rather more detailed information on the nature and time evolution of the conformational fluctuations than does a more conventional large-scattering-volume dynamic light scattering experiment, which gives only *second-order* properties of the scattered field.

We start here with a qualitative description of the principles underlying the experiment; quantitative details are given in section II. Consider first the familiar situation where coherent light is scattered by a large volume V of a solution containing many (noninteracting) rigid spherical particles. As is well-known the intensity scattered by such a solution fluctuates in time due to the changing interference between the light fields scattered by different particles. If D_T is the translational diffusion constant of the particles and K the magnitude of the scattering vector, the typical fluctuation time of the intensity is $(D_T K^2)^{-1}$, roughly the time taken by a particle to diffuse a distance (K^{-1}) equal to the reciprocal of the scattering vector. Furthermore the fluctuations in the scattered light field are only correlated within one "coherence solid angle", $\sim(\lambda/V^{1/3})^2$, where λ is the light wavelength. Thus if two detectors are set in the far field and separated by an angle greater than $\lambda/V^{1/3}$, no cross correlation is observed between their outputs. If the particles are nonspherical and/or flexible, then rotational motions and conformational changes can contribute to fluctuations in the scattered intensity especially when $KR_G \gtrsim 1$, R_G being the particle's radius of gyration. In many cases, however, the time constants of the interference intensity fluctuations caused by rotational and conformational motions are sim-

* Permanent address: Royal Signals and Radar Establishment, Malvern, WR14 3PS, England.

0024-9297/85/2218-1950$01.50/0 Published 1985 by the American Chemical Society